Enhancing structural health monitoring with vehicle identification and tracking

Enhancing Structural Health Monitoring with Vehicle Identification and Tracking

Alessio Burrello
DEI, University of Bologna
Bologna, 40136, Italy
alessio.burrello@unibo.it

Davide Brunelli
DII, University of Trento
Trento, 38123, Italy
davide.brunelli@unitn.it

Marzia Malavisi
Politecnico of Turin
Torino, 10129, Italy
marzia.malvisi@polito.it

Luca Benini
DEI, University of Bologna
IIS, ETH Zurich
lbenini@iis.ee.ethz.ch

***Abstract*—Traffic load monitoring and structural health monitoring (SHM) have been gaining increasing attention over the last decade. However, most of the current installations treat the two monitoring types as separated problems, thereby using dedicated installed sensors, such as smart cameras for traffic load or accelerometers for Structural Health Monitoring (SHM). This paper presents a new framework aimed at leveraging the data collected by a SHM system for a second use, namely, monitoring vehicles passing on the structure being monitored (a viaduct). Our framework first processes the raw three-axial acceleration signals through a series of transformations and extracts its energy. Then, an anomaly detection algorithm is used to detect peaks from 90 installed sensors, and a linear regression together with a simple threshold filters out false detection by estimating the speed of the vehicles. Initial results in conditions of moderate traffic load are promising, demonstrating the detection of vehicles and realistic characterization of their speed. Moreover, a $k-$means clustering analysis distinguishes two groups of peaks with statistically different features such as amplitude and damping duration that could be likely associated with heavy vehicles and cars, respectively.**

***Index Terms*—Structural Health Monitoring, Edge computing, Traffic load monitoring, Anomaly detection.**

I. Introduction

Vehicular traffic is becoming a key factor for ordinary and structural maintenance of roads. Therefore, there is an increasing demand for improved and real-time monitoring of road traffic all over the world. Particularly, bridges and viaducts are essential links in the transportation infrastructure and require such monitoring. This type of analysis usually involves the quantification of the traffic load and the characterization of the passing vehicles [1]. Both these statistics could be of interest for business, e.g. to plan maintenance works and for the monitoring of road conditions, e.g. for bridges'/viaducts' load quantification.

Previous works in this area have exploited camera data and machine learning approaches to quantify the traffic on the roads [2], [3], reaching very high accuracy. In [3], in the period of 23 s, their algorithm correctly identifies 16 cars out of 16 and computes their speeds with a maximum error of 5.3 %. As a counterpart, these methods require dedicated instrumentation, such as an installed camera on the roads, which are expensive to install and maintain in operation [4], even in case of ultra-low power design [5]. Other approaches [6], [7] aim at detecting the traffic load through smartphone sensors, avoiding any installed sensors, but requiring a massive subscription of people to the program (i.e., to share their smartphones' data). Even though this approach could well fit the monitoring of city roads, it is challenging to generalize to highways, where traffic is often long-range and highly diverse.

On the other hand, Structural Health Monitoring (SHM) [8], [9] whose aim is to provide information about roads, bridges, viaducts conditions has been getting growing attention over the last decade. To improve the maintainability of large structures such as space vehicles [10], masonry buildings [11], tunnels [12] or bridges [13], large sensors networks are installed and supervised by local gateways. These monitoring systems continuously acquire and transmit data to a central unit for storage and processing purposes. In this framework, a huge amount of data is collected and available for additional analysis, such as bridges or viaducts traffic monitoring. Moreover, data from installed sensors such as accelerometers, or inclinometers, can also provide joint information about the structural health of the system with respect to an increasing traffic load.

Many studies pave the way to this type of joint considerations by modeling the vibration of bridges under moving vehicles [14], [15], i.e. by identifying relationships between mass, breaking, and speeds and the vibration of the road. Based on these considerations, authors from [16] designed a monitoring traffic system on a railway bridge using four embedded strain transducers. Authors in [17] also review different protocols for SHM using passing vehicles, by exploiting mathematical equations to model the vehicles and their interactions with the bridge.

To tackle the challenge above of installing dedicated sensors or assuming collaborative road users, we propose a framework to leverage already widely diffused SHM installation to further extract information for the data they produce and provide statistics on the passing vehicles. We describe the following contributions:

- We propose a new framework that, starting from a real-life SHM installation, i.e. a large set of acceleration-monitoring

The research is funded by the ST Microelectronics, and partially supported by the EU H2020-ECSEL project AI4DI (g.a. 826060) and by the EU H2020-ECSEL project Arrowhead Tools (g.a. 826452).

nodes installed on a viaduct, extracts statistics about passing vehicles. In sharp contrast with existing methods, our approach does not require any new installation or external source, while using only collected data from the inertial monitoring. Our proposed framework exploits vibration data from network nodes already installed on the tendons of the viaduct to detect, trace, and characterize vehicles on the viaduct. Hence, the incremental cost for getting this additional information is zero.

- We show the benefits of using our processing chain with respect to directly work on raw acceleration data, simultaneously improving the separation between peaks, reducing their duration and removing secondary peaks caused by damping.
- We further investigate the possibility of separate vehicles in different classes, trying to differentiate between light motor and heavy motor vehicles. A simple $k-$means approach is investigated, that leads to create two groups with statistically different behavior.

The rest of the article is organized as follows: Section II introduces the Structural Health Monitoring viaduct installation. Section III presents the main contribution of the paper, i.e. a new framework for recognition and characterization of vehicles on the bridges. Finally, Section IV discusses the initial results, while Section V concludes the paper with final remarks.

II. Structural Health Monitoring Installation

A. Viaduct overview

The monitored structure is a highway concrete bridge located in Italy. In particular, it is a composite box girder in which externally prestressed tendons were used to strengthen the structure. The total length of the viaduct is 580 m and the main girder cross-section height varies from 6.0 m (at the bearings) to 3.0 m (on the center-line of each span). Five concrete piers hold up the five equally space (120 m) hyperstatic spans, and the one isostatic span (43 m long).

External prestressing is provided by unbonded tendons (consisting of 27 strands) that are placed, and prestressed, outside the structure and anchored at the abutments, with several deviators during the length of the structure. For an ideal string without flexural rigidity, the natural frequency of a tendon can be obtained by:

$$f = \frac{n\pi}{L}\sqrt{\frac{T}{\rho}}$$

where n is the mode number of vibration, T the axial force acting on the cable, L the tendon length, and ρ the mass per unit length of the tendon.

The monitored tendons all have approximately the same mass and the same stress in each cable. Regarding the length, tendons belonging to sections 1 to 9 have very similar external strands, with a length of about 20 m. On the contrary, tendons of section 10 have a reduced length of about 7.30 m, due to the closest positioning of the steel deviators. For this reason, the natural vibration frequency of tendons located in section 10 is higher (about 20 Hz) with respect to all the other tendons (about 7-8 Hz).

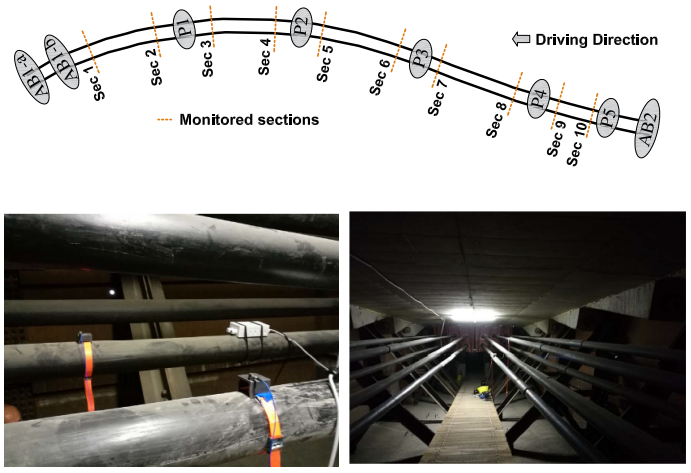

Fig. 1. Monitoring system installation: (1) Plan view of the monitored highway viaduct. (2) MEMS accelerometers installed on the external steel tendons. (3) External prestressing tendons.

TABLE I
Exact number of sensors and spatial localization per each group. The distance is computed from P5, Figure 1

Sections	S10*	S9*	S8*	S7*	S6*
# of Sensors	7	7	6	6	9
distance [m]	0.0 m	67.0 m	75.0 m	187.0 m	195.5 m
Sections	S5*	S4*	S3*	S2*	S1*
# of Sensors	11	10	10	12	12
distance [m]	307.5 m	316.0 m	428.0 m	436.5 m	548.5 m

The structural safety of a prestressed bridge is highly dependent on the durability of its prestressing tendons. In this regard, corrosion by aggressive water-borne agents could seriously compromise the health of steel tendons, causing the deterioration or failure of these elements.

In recent years, the structure experienced the failure of one tendon, which highlighted the need to monitor the health condition of prestressed elements during the service life of the viaduct. For this reason, a continuous monitoring system was installed between June and September 2017 for the real-time detection of the tendons' behavior over time. The complete system is then fully active since 20 September 2017.

B. Sensors installation

The viaduct has been equipped with a real-time monitoring system to analyze the dynamic response of the structure under operational conditions, as described in [18]. External tendons were thus instrumented with 90 MEMS tri-axial accelerometers, 2 for each monitored element, with a sampling frequency of 100 Hz. Triaxial MEMS accelerometers measure the linear acceleration in

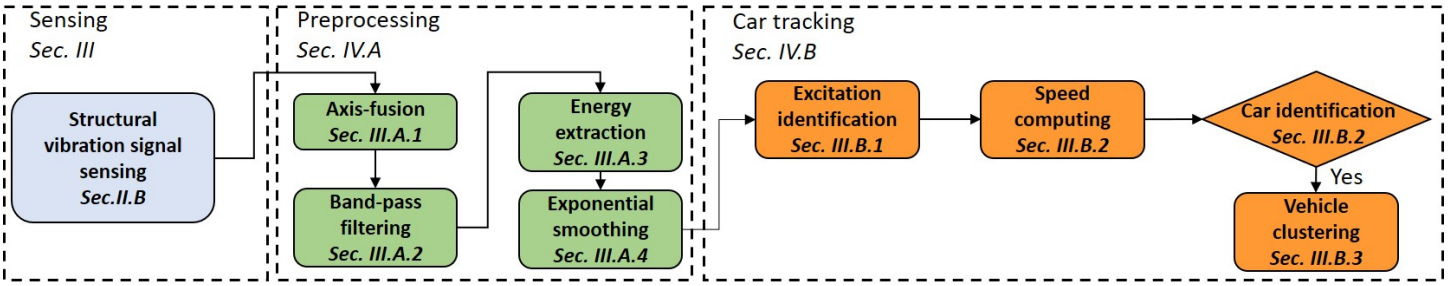

Fig. 2. The processing chain of our algorithm: (1) 90 3-axis accelerometers extract the acceleration of the viaduct in different points. (2) A series of transformations and feature extractions are applied to transform the raw signal in a 1D meaningful trace. (3) Anomaly detection algorithms and regression methods are applied to track vehicles on the viaduct. Further, a cluster analysis tries to characterize the vehicles in two different groups, targeting the distinction between light motor vehicles and heavy motor ones.

three orthogonal directions (x, y, z), assuming an angle between each two of those directions of $90° \pm 2\%$.

To prevent aliasing, data are sampled at the sensor level at 25.6 kHz and then filtered and downsampled at the sensor node at 100 Hz; in this way, the data streaming becomes manageable by the network [19], [20].

The accelerometers were placed in the upper part of the prestressing cables in 10 different cross-sections, close to the piers and abutments, as shown in Figure 1. The viaduct carries traffic in the northbound direction, from section number 10 to section number 1. The number of sensors for each instrumented section is not constant along the viaduct; indeed, every section can have from six to twelve sensors recording accelerations under traffic excitations. This allows considering "sensors groups" as each group containing all sensors recording the same type of acceleration in the same section of the viaduct. Table I depicts the exact number of sensors and the exact distance from the beginning of the viaduct for each group.

Noteworthy, the sensors groups' positions were decided prior to and independently from the conduction of these experiments and with the primary scope of monitor the structural health of the viaduct. The installation of the nodes on the tendons is probably not optimal for car traffic monitoring, which could benefit from sensors installed directly in the roadway infrastructure. However, our goal is to demonstrate that sensors positioned for SHM can be used with a second purpose to monitor vehicular traffic.

Each sensor, representing a node of the monitoring system, includes a microcontroller providing data sampling and some basic management operations. After reading accelerations, sensors encode the sampled data into a CAN-BUS driven network, joining and transmitting data to a local gateway, where they are stored and pre-processed. From gateways, data are sent to a specific IoT Cloud platform in real-time.

III. Algorithm: Car Identification & Tracking

In this section, we present the main contribution of the paper, namely a framework to identify, trace, and characterize vehicles on a viaduct starting from acceleration signals. First, we show how different preprocessing techniques and feature extractors can be combined to encode a 2D vibration signal in a smooth trace that better highlights passing vehicles. Then, a signal anomaly detection algorithm is applied to recognize vehicles' passages. Note that we use the anomaly detection to distinguish between acceleration signals of the tendons of the viaduct during a null traffic load period (= normal windows) and accelerations with peaks derived from passing vehicles or other events (= anomalous windows). Finally, linear regression and K-means clustering are applied to estimate the speeds of the vehicles and to provide a differentiation of the vehicles that go across the viaduct. Furthermore, we use computed speeds to filter out anomalous windows associated with environmental conditions or to instrumentation problems. Figure 2 describes the whole framework, comprising Sensing part (Section II), Preprocessing (Section III-A), and Car tracking (Section III-B)

A. Preprocessing & feature extraction

The preprocessing module first fuses the accelerations of the two vibration axis, i.e. x and z. The vibration of the tendons has an elliptical shape on the xz plane, implying that both axis accelerations are necessary to account for the overall vibration correctly. Then, a bandpass filter reduces the long damping of low-frequency vibrations. Since peaks generated by vehicles are a mixture of different frequencies, we maintain only the highest visible one, thus enhancing the separation of peaks derived from near passing vehicles. Finally, the energy is extracted and smoothed in a 1-second shifting window without overlap as markers of the traffic on the viaduct. This signal is sent to the car tracking module and in particular, to the anomaly detection algorithm to recognize vehicle passages. In the next sections, every single block of the preprocessing module (Figure 3) is described in detail.

1) L_2 normalization: To capture the two-dimensional vibration of the tendons, the L_2 normalization is applied to fuse the data from the two axes of the vibration plane, i.e. xz plane. L_2 normalization is computed as follow:

$$|\cdot|_{L_2} = \sqrt{(x-\overline{x})^2 + (z-\overline{z})^2}$$

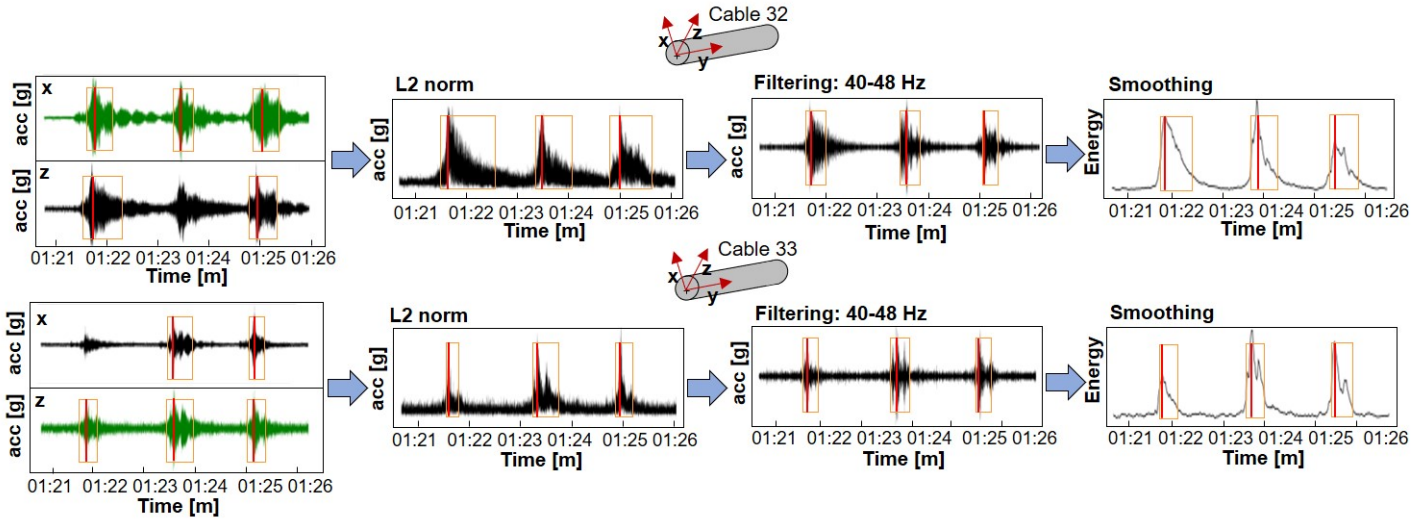

Fig. 3. From left to right: (1) Acceleration on two different cables on the x-z plane as measured by the accelerometers. (2) L_2 normalization of the signal to merge the two traces. (3) Fourth-order Butterworth bandpass filter application to eliminate low frequencies dampings. (4) Energy extraction and exponential smoothing filter ($\alpha = 0.7$) application. Orange boxes delimit all the anomalous windows as identified by the anomaly detection algorithm of Section III-B1, whereas red thick vertical lines identify the window with the highest energy among consecutive anomalous windows.

where $\overline{x}$ and $\overline{z}$ stand for the mean of the axis during a reference period of 5 minutes free of peaks. The first two panels of Figure 3 highlight the benefits of axes fusion. For two different cables, the L_2 normalization leads to correctly identify 3 peaks, whereas using separated axes, we miss a peak on the z (Cable 32) and a peak on the x axis (Cable 33).

2) 4^{th} order Butterworth filter: A bandpass filter is applied to reduce the damping time of the peaks. This step is added to the chain to better separates peaks that are very close in the time axis, whose damping can cause an almost total overlap. Since higher frequencies present faster damping, we decide to maintain only the highest informative frequency. As presented in Section II, the tendons vibrate at a natural frequency of $\sim$8 Hz and at its multiples [21]. A spectrogram analysis further confirms this consideration, showing the peaks of vibration of the viaduct on multiples of natural frequency. Hence, a 4^{th} order bandpass Butterworth filter between 40 Hz and 49 Hz is applied, thereby including a single multiple of the natural frequency, i.e. $\sim$40 Hz. Note that higher frequencies cannot be detected since we acquire data at 100 Hz sampling frequency. As can be seen in panels 3 of Figure 3, the filter considerably reduces the damping time, by better isolating the peaks. In the figure, orange boxes indicate the beginning and the end of the peaks as delimited by our approach described in Section III-B1.

3) Energy extraction: The energy is computed starting from the filtered acceleration as

$$E = \sum_{t=0}^{100} S_i^2$$

during each 1 second shifting window. We empirically choose one second as the window size to ensure that the beginning part of the vehicle vibration signal is detected as well as to filter out isolated peaks caused by instrumentation's defects.

4) Exponential smoothing: Finally, we apply the exponential smoothing to the extracted energy. This filter helps in the reduction of the oscillation amplitude during damping by taking into account the history of the signal. Note that a high oscillation amplitude can cause lots of isolated and not consecutive windows to be labeled as anomalous by the approach described below and to be incorrectly identified by the tracking algorithm as different vehicles. Mathematically, this second filter is represented as

$$E[t] = \alpha * E[t] + (1 - \alpha) * E[t-1]$$

with E the energy and α the smoothing factor. In this work, we set $\alpha = 0.7$. The last panel of Figure 3 shows the smoothed extracted energy from the accelerometers data.

B. Car tracking & clustering

The Car tracking module is organized into three blocks: (1) The first block, i.e. the excitation identification, exploits an anomaly detection algorithm to identify the peaks associated with vehicles on the bridge. (2) The second one leverages the previous detection to identify the exact time of passage over the sensor. This block further combines the detection times of each sensor through a linear regression analysis to compute the speed of the vehicles. (3) The final block exploits 5 different features computed on each identified peak through a $k-$means clustering algorithm, to identify two groups of vehicles, likely light motor, and heavy motor vehicles.

1) Anomaly detection: car identification: A Gaussian model has been fitted to identify anomalies in the input signal (i.e. the smoothed energy). As explained, we consider passing vehicle

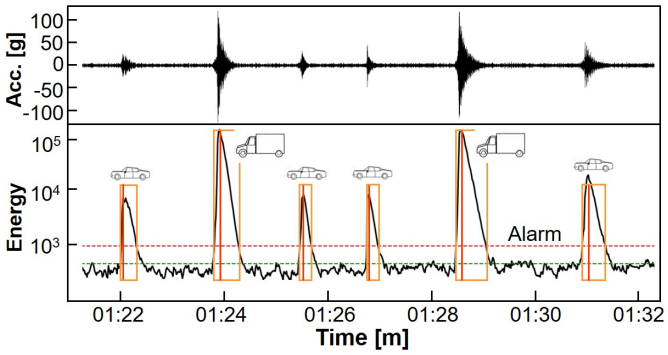

Fig. 4. In the top panel, normalized and filtered acceleration from Sensor 1D30. The bottom panel depicts the corresponding smoothed energy and the vehicles detection. Highest peaks imply heavier motor vehicles.

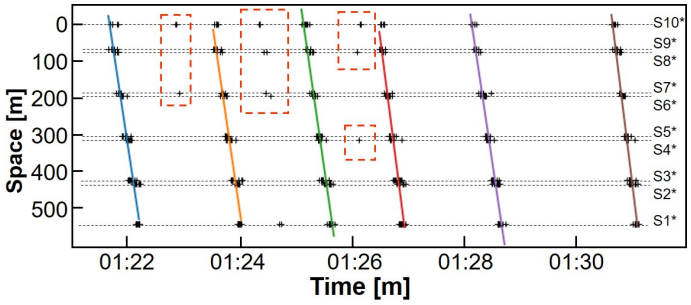

Fig. 5. Trajectory of the six vehicles depicted in Figure 4 using the detection of all the 90 sensors. + indicates the detection time of each sensor, whereas colored lines show the linear regression among all the samples belonging to a trace. Red dotted squares contain filtered single prediction errors.

vibration peaks as anomalies and null traffic load as a normal condition. A window of 15 minutes free of peaks is initially used to set the parameters of the Gaussian, namely, mean and standard deviation. After, the mean and the standard deviation are updated over time with labeled "normal" 1-second windows as

$$\overline{G} = \frac{1-i}{i}\overline{G} + \frac{1}{i}\overline{E_i} \mid i \in \{\text{normal windows}\}$$

$$\sigma(G) = \frac{1-i}{i}\sigma(G) + \frac{1}{i}\sigma(E_i) \mid i \in \{\text{normal windows}\}$$

To recognizes anomalies (i.e. passing vehicles), the energy E_i of each new 1 second window is compared with our fitted model: $E_i > \overline{G} + thr$ identifies the presence of an anomaly. Based on the Gaussian probability density function

$$P\{\overline{G} - 3\sigma(G) < E_i < \overline{G} + 3 \times \sigma(G)\} = 99,7\%$$

we set $thr = 3 \times \sigma(G)$ to achieve only 0.3% false positive detections. Note that all consecutively identified anomalies are grouped and correspond to unique vehicle identification. Two consecutive windows labeled as N-A, where A is an anomalous window and N a normal one, correspond to the beginning of a vehicle caused vibration, whereas a sequence of the form A-N, corresponds to the end of the vibration. Hence, an anomaly detection of the form AA-NN-A-N-AAA-N is associated with the passage of 3 vehicles, whereas one of the form N-AAAAAAAA-N encodes a single passing vehicle. Figure 4 depicts the identification of six vehicles during a 10 minutes window on the night of the 18th of February 2018. The orange boxes contain all the windows labeled as anomalous by our approach, i.e. windows that likely correspond to the passage of a vehicle. Importantly, this algorithm runs separately for every single sensor, thereby producing a different set of detection for each of them.

2) Linear regression for speed computation: To compute the speed of the vehicles and filter out the peaks caused by environment and/or sensors' defects, we distribute the sensor and their detection times on a time-space graph based on the sensor positions reported in Table I of Section II and we recognize sensor detections belonging to vehicles, i.e. detections that belong to realistic traces. First, we fix the exact *show* point of the vehicles on each sensor as the sample with the highest energy in the detection window (time period composed by consecutive anomalous 1-second windows identifications) previously identified and we associate to each sensor its distance from the beginning of the viaduct. Then a linear regression is applied, and the mean speed of vehicles is computed as the first temporal derivative of the regression. We separate each vehicle trace, by selecting the starting point from S10* sensors (entrance of the viaduct) and then the nearest detection point for every single sensor. Noteworthy, we filter out fake vehicles identifications by eliminating traces that result in a speed $> 200\,\mathrm{km/h}$ (e.g. synchronous sensor reset defects) and single sensor detection errors with any detection points in the next span during the 10 second after (theoretical speed $< 50\,\mathrm{km/h}$). Figure 5 depicts the identification of the 6 vehicles from the previous figure, but among all the 90 sensors. Importantly, all the speeds computed are comprised between 65 km/h and 95 km/h. The red dotted squares show some false detection filtered out by our approach.

3) Vehicles separation: $k-$means clustering: Finally, we exploit some simple statistical features and an unsupervised approach, i.e. the $k-$means clustering [22], to propose a grouping of the different peaks extracted by our anomaly detection algorithm. Five different simple features have been selected, namely the maximum amplitude of the peak, its duration, the mean energy, the line length [23], and the standard deviation. Their joint signal characterization motivates the choice of these features. Then, a $k-$means clustering analysis with $k = 2$ is fitted on them to separate the peaks in two groups. The $k-$means is an iterative approach that begins by randomly selecting k centroids in the input space and by assigning each input point to the nearest centroid. Then, at each successive step, the centroids are updated as the barycenters of their assigned points, and all the points are again classified. This process continues until no more changes are done in the positions of the centroids.

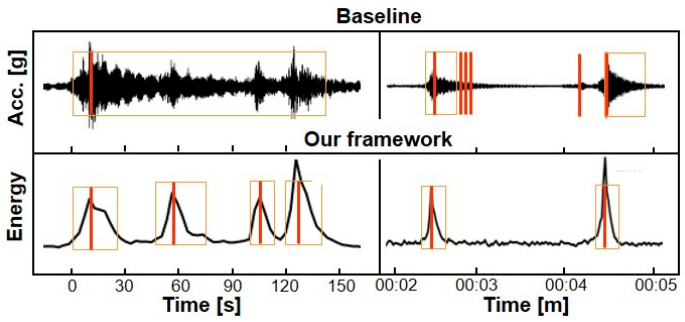

Fig. 6. Comparison of our framework with a baseline approach on three different critical situations, namely near peaks, long damping peaks, and high oscillating damping. Again, orange boxes and red lines identify boxes of peak detection and exact time of the peaks.

TABLE II
ANALYSIS OF THE TWO CLUSTERS IDENTIFIED BY THE K-MEANS CLUSTERING. ABBREVIATIONS: MI.:MINIMUM, MA.: MAXIMUM, N.A.:NOT APPLICABLE, A.: MAXIMUM AMPLITUDE, E.: ENERGY, L.L.: LINE LENGTH, STD.: STANDARD DEVIATION.

Features	Cluster 1		Cluster 2		t-test*	$p-$value
	Mean	[Mi,Ma]	Mean	[Mi,Ma]		
# peaks	214	n.a.	119	n.a.	n.a	n.a.
A. [g]	108.9	[31,283]	467.8	[297,942]	yes	<0.0001
time [s]	15.4	[1,69]	68.5	[22,281]	yes	<0.0001
E.	29.3	[11,86]	66.4	[41,120]	yes	<0.0001
L.l.	15.0	[6,40]	47.3	[30,83]	yes	<0.0001
Std	13.7	[6,39]	31.0	[15,65]	yes	<0.0001

* statistically significant at 1% level

IV. RESULTS

To initially evaluate the validity of our framework, we analyze some critical situations such as near peaks and long damping peaks by showing the benefits of applying the above described processing chain with respect to directly predict anomalies on the raw signal, i.e. to predict an anomaly every time the σ of the acceleration is higher than three times the noise σ – measured on a reference period of 15 minutes without peaks and continuously updated as previously explained in Section III-B1. Figure 6 depicts the comparison of the two methods. We first compare the predictions on near acceleration peaks: our approach correctly separates the four peaks, by reducing the damping of low frequencies with the bandpass filter. Conversely, the detection of raw signals groups all the peaks in a single detection box, thereby losing 3 vehicles out of 4. Furthermore, for long damping peaks (right part of Figure 6), the bandpass filter and the smoothing filter introduced in our approach lead to correct single peak identifications by reducing the damping time and oscillation, whereas working on the raw signals causes multiple vehicle detections during the damping oscillations.

We also analyze the speeds of vehicles on the viaduct during a low traffic load period. We compute the speeds of different vehicles during nights' hours: all the measures are comprised in the range $[60\,\mathrm{km}, 105\,\mathrm{km}]$. Some examples of this computation are depicted in Figure 5.

Finally, we assess the proposed distinction of the detected peaks by a clustering approach. A $k-$means analysis with $k = 2$ has been exploited for the creation of two groups, likely light motor vehicles, and heavy motor vehicles. We evaluate this approach on five nights – low traffic load condition – for a total of 333 detected peaks on a single sensor. Table II deeply compares the two generated groups entailing, respectively 214 and 119 peaks. In at-student test, all the extracted features are significantly different between the two groups, resulting in a $p-$value < 0.0001. Noteworthy, Cluster 2 presents a lower number of peaks with higher amplitude and damping time and is probably associated with a group of heavy motor vehicles.

V. CONCLUSIONS

This work presents a new approach to enhance SHM bridge/viaduct installations with new statistics about the traffic load without adding further sensors. We detail the instrumentation of an SHM installation on a real standing viaduct, firstly aimed at studying its structural condition and exploited by our framework to study the traffic conditions and gives information about the vehicles passing through the viaduct. The results achieved from the few tests that have been conducted so far show the potential to provide traffic load information and traffic diagnosis. We also show a totally unsupervised approach to classify passing vehicles. Our future work will focus on validating our results with video observations and on applying our method to day times, characterized by higher traffic density and hence, more challenging.

REFERENCES

[1] T. Seo, A. M. Bayen, T. Kusakabe, and Y. Asakura, "Traffic state estimation on highway: A comprehensive survey," Annual Reviews in Control, vol. 43, pp. 128 – 151, 2017.

[2] D. Sitaram, N. Padmanabha, Supriya S, and Shibani S, "Still image processing techniques for intelligent traffic monitoring," in 2015 Third International Conference on Image Information Processing (ICIIP), Dec 2015, pp. 252–255.

[3] K. Song and J. Tai, "Image-based traffic monitoring with shadow suppression," Proceedings of the IEEE, vol. 95, no. 2, pp. 413–426, Feb 2007.

[4] I. Y. Gu and M. Bolbat, "Road traffic tracking and parameter estimation based on visual information analysis using self-calibrated camera views," in 2013 Seventh International Conference on Distributed Smart Cameras (ICDSC), Oct 2013, pp. 1–6.

[5] M. Nardello, H. Desai, D. Brunelli, and B. Lucia, "Camaroptera: A batteryless long-range remote visual sensing system," in Proceedings of the 7th International Workshop on Energy Harvesting & Energy-Neutral Sensing Systems. New York, NY, USA: Association for Computing Machinery, 2019, p. 814. [Online]. Available: https://doi.org/10.1145/3362053.3363491

[6] P. Mohan, V. Padmanabhan, and R. Ramjee, "Nericell: Rich monitoring of road and traffic conditions using mobile smartphones," in ACM Sensys. Association for Computing Machinery, Inc., November 2008, raleigh, NC, USA.

[7] R. Bhoraskar, N. Vankadhara, B. Raman, and P. Kulkarni, "Wolverine: Traffic and road condition estimation using smartphone sensors," in 2012 Fourth International Conference on Communication Systems and Networks (COMSNETS 2012), Jan 2012, pp. 1–6.

[8] A. Abdelgawad and K. Yelamarthi, "Structural health monitoring: Internet of things application," in 2016 IEEE 59th International Midwest Symposium on Circuits and Systems (MWSCAS), Oct 2016, pp. 1–4.

[9] C. A. Tokognon, B. Gao, G. Y. Tian, and Y. Yan, "Structural health monitoring framework based on internet of things: A survey," IEEE Internet of Things Journal, vol. 4, no. 3, pp. 619–635, June 2017.

[10] M. Hedley, N. Hoschke, M. Johnson, C. Lewis, A. Murdoch, D. Price, M. Prokopenko, A. Scott, P. Wang, and A. Farmer, "Sensor network for structural health monitoring," in Proceedings of the 2004 Intelligent Sensors, Sensor Networks and Information Processing Conference, 2004., Dec 2004, pp. 361–366.

[11] C. Ayyildiz, H. E. Erdem, T. Dirikgil, O. Dugenci, T. Kocak, F. Altun, and V. C. Gungor, "Structure health monitoring using wireless sensor networks on structural elements," Ad Hoc Networks, vol. 82, pp. 68 – 76, 2019.

[12] D. Porcarelli, D. Spenza, D. Brunelli, A. Cammarano, C. Petrioli, and L. Benini, "Adaptive rectifier driven by power intake predictors for wind energy harvesting sensor networks," IEEE Journal of Emerging and Selected Topics in Power Electronics, vol. 3, no. 2, pp. 471–482, June 2015.

[13] M. Reyer, S. Hurlebaus, J. Mander, and O. E. Ozbulut, "Design of a wireless sensor network for structural health monitoring of bridges," in 2011 Fifth International Conference on Sensing Technology, Nov 2011, pp. 515–520.

[14] F. T. K. Au, Y. S. Cheng, and Y. K. Cheung, "Vibration analysis of bridges under moving vehicles and trains: an overview," Progress in Structural Engineering and Materials, vol. 3, no. 3, pp. 299–304, 2001. [Online]. Available: https://onlinelibrary.wiley.com/doi/abs/10.1002/pse.89

[15] T. Vaidya and A. Chatterjee, "Vibration of road bridges under moving vehicles: a comparative study between single contact point and two contact point models," Transactions of the Canadian Society for Mechanical Engineering, vol. 41, no. 1, pp. 99–111, 2017.

[16] R. Karoumi, J. Wiberg, and A. Liljencrantz, "Monitoring traffic loads and dynamic effects using an instrumented railway bridge," Engineering Structures, vol. 27, no. 12, pp. 1813 – 1819, 2005, sEMC 2004 Structural Health Monitoring, Damage Detection and Long-Term Performance.

[17] A. Malekjafarian, P. J. McGetrick, and E. J. OBrien, "A review of indirect bridge monitoring using passing vehicles," Shock and vibration, vol. 2015, 2015.

[18] A. Girolami, D. Brunelli, and L. Benini, "Low-cost and distributed health monitoring system for critical buildings," in 2017 IEEE Workshop on Environmental, Energy, and Structural Monitoring Systems (EESMS), July 2017, pp. 1–6.

[19] A. Burrello, A. Marchioni, D. Brunelli, and L. Benini, "Embedding principal component analysis for data reduction in structural health monitoring on low-cost iot gateways," in Proceedings of the 16th ACM International Conference on Computing Frontiers, ser. CF 19. New York, NY, USA: Association for Computing Machinery, 2019, p. 235239.

[20] A. Girolami, F. Zonzini, L. De Marchi, D. Brunelli, and L. Benini, "Modal analysis of structures with low-cost embedded systems," in 2018 IEEE International Symposium on Circuits and Systems (ISCAS), May 2018, pp. 1–4.

[21] E. Hamed and Y. Frostig, "Natural frequencies of bonded and unbonded prestressed beams–prestress force effects," Journal of sound and vibration, vol. 295, no. 1-2, pp. 28–39, 2006.

[22] J. MacQueen, "Some methods for classification and analysis of multivariate observations," in 5th Berkeley Symposium on Mathematical Statistics and Probability, 1967.

[23] L. Guo, D. Rivero, J. Dorado, J. R. Rabual, and A. Pazos, "Automatic epileptic seizure detection in eegs based on line length feature and artificial neural networks," Journal of Neuroscience Methods, vol. 191, no. 1, pp. 101 – 109, 2010.